J|A|C|S ARTICLES

Published on Web 01/20/2010

Reaction Mechanisms of the Multicopper Oxidase CueO from *Escherichia coli* Support Its Functional Role as a Cuprous Oxidase

Karrera Y. Djoko,[#] Lee Xin Chong, Anthony G. Wedd, and Zhiguang Xiao*

School of Chemistry and Bio21 Molecular Science and Biotechnology Institute, University of Melbourne, Parkville, Victoria 3010, Australia

Received October 29, 2009; E-mail: z.xiao@unimelb.edu.au

Abstract: CueO from *Escherichia coli* is a multicopper oxidase (MCO) involved in copper tolerance under aerobic conditions. It features four copper atoms that act as electron transfer (T1) and dioxygen reduction (T2, T3; trinuclear) sites. In addition, it displays a methionine-rich insert which includes a helix that blocks physical access to the T1 site and which provides an extra labile site T4 adjacent to the T1 center. This T4 site is required for CueO function. Like many MCOs, CueO exhibits phenol oxidase activity with broad substrate specificity. Maximal activity with model substrate 2,6-dimethoxyphenol required stoichiometric occupation of T4 by Cu^{II} (notation: Cu^{II}-CueO). This was achieved in Mops buffer which has little affinity for Cu^{2+}. However, pH buffers that bind or precipitate Cu^{2+} (Tris, BisTris, and KPi) generated enzyme with a vacant T4 site (notation: □-CueO) which has no phenol oxidase activity. Addition of excess Cu^{2+} effectively generated a Cu^{2+} buffer and recovered the activity partially or completely, depending upon the specific pH buffer. This phenomenon allowed reliable estimation of the affinity of T4 for Cu^{II}: $K_D = 5.5 \times 10^{-9}$ M. CueO is involved in copper tolerance and has been suggested to be a cuprous oxidase. The anion $[Cu^{I}(Bca)_2]^{3-}$ (Bca = bicinchoninate) acted as a novel chromophoric substrate. It is a robust reagent, being air-stable and having a Cu^{I} affinity comparable to those of periplasmic Cu^{I} binding proteins. The influences of pH buffer composition and of excess Cu^{2+} on cuprous oxidation were diametrically opposite to those seen for phenol oxidation, suggesting that □-CueO, not Cu^{II}-CueO, is the resting form of the cuprous oxidase. Steady-state kinetics demonstrated that the intact anion $[Cu^{I}(Bca)_2]^{3-}$, not "free" Cu^{+}, is the substrate that donates Cu^{I} directly to T4. The data did not follow classical Michaelis−Menten kinetics but could be fitted satisfactorily by an extension that considered the effect of free ligand Bca. The K_m term consists of two components, allowing estimation of the transient affinity of T4 for Cu^{I}: $K_D = 1.3 \times 10^{-13}$ M. It may be concluded that Cu^{I} carried by $[Cu^{I}(Bca)_2]^{3-}$ is oxidized only upon complete transfer of Cu^{I} to T4. The transfer is required to induce a negative shift in the copper reduction potential to allow oxidation and electron transfer to the T1 site. The results provide compelling evidence that CueO is a cuprous oxidase. The new approach will have significant application to the study of metallo-oxidase enzymes.

Introduction

CueO is a multicopper oxidase (MCO) expressed to the periplasmic space in *Escherichia coli*. CueO and the membrane-bound Cu^{I}-translocating P-type ATPase CopA constitute a copper efflux system that confers copper tolerance under aerobic conditions.[1] Expression of both enzymes is upregulated in response to copper stress by the cytosolic metalloregulatory protein CueR.[2]

Like all MCOs, CueO features three copper sites, T1, T2, and binuclear T3 (blue, cyan, and purple spheres, respectively, in Figure 1).[3−5] It couples four one-electron substrate oxidation steps to the four-electron reduction of dioxygen to water.[3,6] The T1 site generally catalyzes substrate oxidation, and the T2, T3 trinuclear copper cluster catalyzes dioxygen reduction. However, CueO is unusual: it displays an extra methionine-rich insert which includes a helix that blocks physical access to the T1 center and which provides an extra labile copper site essential for phenol oxidase activity.[4,7,8] This site is only 7.5 Å away from the T1 center and is linked to T1 through a hydrogen bond (Figure 1b).[7] It is labeled T4 in this work (red sphere in Figure 1).

[#] Present address: School of Chemistry and Molecular Biosciences, University of Queensland, St Lucia 4072, Australia.

(1) Rensing, C.; Grass, G. *FEMS Microbiol. Rev.* **2003**, *27*, 197–213.
(2) Outten, F. W.; Outten, C. E.; Hale, J.; O'Halloran, T. V. *J. Biol. Chem.* **2000**, *275*, 31024–31029.
(3) Solomon, E. I.; Sundaram, U. M.; Machonkin, T. E. *Chem. Rev.* **1996**, *96*, 2563–2606.
(4) Roberts, S. A.; Weichsel, A.; Grass, G.; Thakali, K.; Hazzard, J. T.; Tollin, G.; Rensing, C.; Montfort, W. R. *Proc. Natl. Acad. Sci. U.S.A.* **2002**, *99*, 2766–2771.
(5) Quintanar, L.; Stoj, C.; Taylor, A. B.; Hart, P. J.; Kosman, D. J.; Solomon, E. I. *Acc. Chem. Res.* **2007**, *40*, 445–452.
(6) Solomon, E. I.; Augustine, A. J.; Yoon, J. *Dalton. Trans.* **2008**, 3921–3932.
(7) Roberts, S. A.; Wildner, G. F.; Grass, G.; Weichsel, A.; Ambrus, A.; Rensing, C.; Montfort, W. R. *J. Biol. Chem.* **2003**, *278*, 31958–31963.
(8) Kataoka, K.; Komori, H.; Ueki, Y.; Konno, Y.; Kamitaka, Y.; Kurose, S.; Tsujimura, S.; Higuchi, Y.; Kano, K.; Seo, D.; Sakurai, T. *J. Mol. Biol.* **2007**, *373*, 141–152.

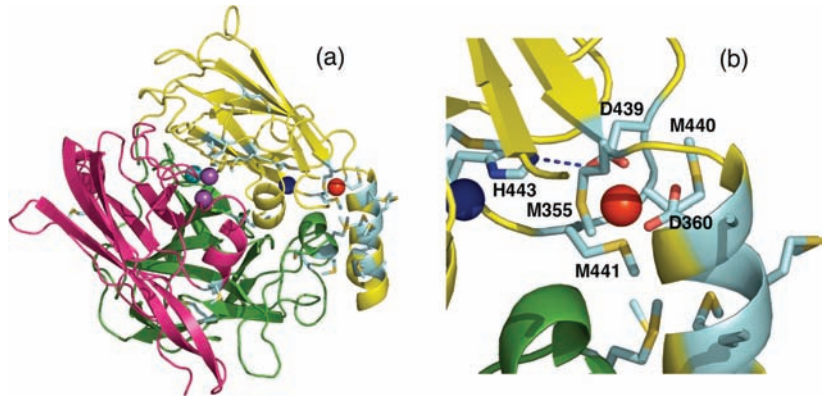

Figure 1. Ribbon representation of the CueO molecule (PDB code 1N68). (a) Overall structure highlighting three structural domains (D1, red; D2, green; D3, gold), four defined copper centers (T1, blue; T2, teal; T3 (binuclear), purple; T4, red), and the location of methionine residues (in gray-yellow sticks). (b) Molecular structure around T4 highlighting the ligands for Cu^{II}, possible ligands for Cu^{I} (including M440), and a hydrogen bond connecting the T4 copper ligand D439 and the T1 copper ligand H443.

CueO functions only in the presence of dioxygen, consistent with its role as an oxidase.[9] Like most MCOs, it exhibits a broad substrate specificity for organic molecules such as catechols, iron-chelating siderophores, and the chromophoric model substrate 2,6-dimethoxyphenol (DMP), and so it was proposed to play a role as a phenol oxidase in copper tolerance.[10−12] These activities are low but are enhanced considerably in the presence of added Cu^{2+}. It has been suggested that effective communication between the buried T1 copper site and the organic substrates requires a Cu^{II} in the T4 site to serve as an electron-transfer mediator.[8,11,12] Consistent with this model, deletion of the methionine-rich insert that isolates the T1 site from the solvent allows direct access of organic substrates to the T1 site, promoting the phenol oxidase activities without the need for added Cu^{2+}.[8]

CueO also possesses cuprous oxidase activity *in vitro* and catalyzes air oxidation of the complex $[Cu^{I}(MeCN)_4]^+$ in aqueous buffer containing ~5% MeCN as a stabilizing ligand.[13] It was reported that excess Cu^{2+} (1 mM) was required in the reaction buffers to stimulate the cuprous oxidase activity, presumably to ensure optimal occupation by Cu^{II} of the T4 site. This implies an outer-sphere mechanism for cuprous oxidation, related to that proposed for phenol oxidation.[8,13] The related enzyme McoA from the hyperthermophilic bacterium *Aquifex aeolicus* also requires added Cu^{2+} for cuprous oxidase activity.[14]

In contrast to its effect on phenol oxidase activity, deletion of the Met-rich insert in CueO decreased cuprous oxidase activity considerably.[8] In addition, we have demonstrated that PcoA, a related MCO involved in copper resistance in *E. coli*, catalyzes air oxidation of selected Cu^{I}-binding proteins in the absence of additional Cu^{2+}.[15]

It is apparent that the reaction mechanisms of these MCOs as phenol oxidases and cuprous oxidases remain controversial and indecipherable. The true physiological roles of CueO and related MCOs in copper homeostasis remain unknown, as do their natural substrates. Using novel approaches, the present work has estimated the affinities of the T4 site for both Cu^{I} and Cu^{II} and identified distinctly different roles for the site in phenol and cuprous oxidation. The results provide compelling evidence that CueO is a cuprous oxidase *in vivo* and not a phenol oxidase. The new approaches have potential for application to study of reaction mechanisms of the metallo-oxidase enzymes responsible for cuprous, ferrous, and manganous oxidation.[5]

Results and Discussion

Protein Expression and Purification. CueO protein has been expressed with an intact 28-residue N-terminal signal for periplasmic translocation and a C-terminal tag for affinity purification.[12] The former was removed after export via the TAT translocation pathway. In the present work, the *cueO* gene was cloned without either addition. The mature protein (488 aa; 53.4 kDa) was overexpressed in *E. coli* cells. Purification by anion exchange followed by size exclusion chromatography led to the isolation of pure *apo*-CueO (>95%) in a yield of ca. 50 mg per liter of culture. ESI-QTOF-MS revealed a molar mass of 53420.5 Da (Figure S1, Supporting Information), consistent with the value of 53420.4 Da predicted from the mature CueO protein sequence without the N-terminal Met residue that was introduced as the initialization codon.

Copper Incorporation and Content. Incubation of *apo*-CueO with excess $CuSO_4$ (10 equiv) in Mops buffer (pH 7) in the presence of GSH (1 mM) at 4 °C led to incorporation of copper ions. Removal of unbound copper and GSH on a desalting column in BisTris-HCl buffer (10 mM, pH 7) produced a blue solution of CueO enzyme which exhibited absorption maxima at 610 nm (ϵ = 5000 M^{-1} cm^{-1}) and 330 nm (ϵ = 4000 M^{-1} cm^{-1}), characteristic of blue T1 and binuclear T3 copper centers, respectively (Figure 2a). Copper analysis confirmed 4.2(3) equiv of copper based on protein concentrations estimated from the absorbance at 610 nm (Table 1). This form contains intact T1, T2, and T3 copper centers but a vacant T4 site (designated here as □-CueO).

Equivalent procedures with Mops (50 mM, pH 7) as the desalting column buffer generated a solution spectrum with essentially identical absorption ratio A_{280}/A_{610} = 11.6 but with more intense relative absorbances around 700 and 330 nm (Figure 2b and inset; Table 1). Copper analysis under the same conditions provided 6.3(3) equiv of copper (Table 1). This form

(9) Outten, F. W.; Huffman, D. L.; Hale, J. A.; O'Halloran, T. V. *J. Biol. Chem.* **2001**, *276*, 30670–30677.
(10) Grass, G.; Thakali, K.; Klebba, P. E.; Thieme, D.; Muller, A.; Wildner, G. F.; Rensing, C. *J. Bacteriol.* **2004**, *186*, 5826–5833.
(11) Kim, C.; Lorenz, W. W.; Hoopes, J. T.; Dean, J. F. *J. Bacteriol.* **2001**, *183*, 4866–4875.
(12) Grass, G.; Rensing, C. *Biochem. Biophys. Res. Commun.* **2001**, *286*, 902–908.
(13) Singh, S. K.; Grass, G.; Rensing, C.; Montfort, W. R. *J. Bacteriol.* **2004**, *186*, 7815–7817.
(14) Fernandes, A. T.; Soares, C. M.; Pereira, M. M.; Huber, R.; Grass, G.; Martins, L. O. *FEBS J.* **2007**, *274*, 2683–2694.
(15) Djoko, K. Y.; Xiao, Z.; Wedd, A. G. *ChemBioChem* **2008**, *9*, 1579–1582.

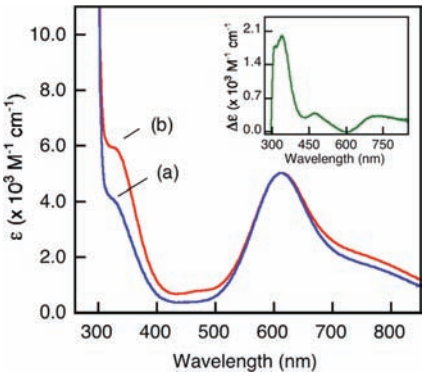

Figure 2. Solution spectra of CueO enzyme (~40 μM) in Mops buffer activated in the presence of excess Cu^{2+} (10 equiv) and isolated on a desalting column: (a) as □-CueO in BisTris-HCl buffer (50 mM, pH 7.0); (b) as Cu^{II}-CueO in Mops buffer (50 mM, pH 7.0). Inset: Spectral difference between Cu^{II}-CueO and □-CueO.

Table 1. Characterization Data at pH 7 for CueO as a Phenol Oxidase (Cu^{II}-CueO) and as a Cuprous Oxidase (□-CueO)

	function	
	phenol oxidase (Mops buffer)	cuprous oxidase (BisTris buffer)
A_{280}/A_{610}	11.6 ± 0.5	11.6 ± 0.5
A_{330}/A_{610}	1.2 ± 0.1	0.8 ± 0.1
Cu/CueO[a]	6.3 ± 0.3	4.2 ± 0.3
Cu^{II} K_D of T4[b]	5.5×10^{-9} M	
Cu^{I} K_D of T4[c]	1.3×10^{-13} M	
$E_{1/2}$ for T4 Cu[d]	+0.42 V vs SHE	
$E_{1/2}$ for T1 Cu[e]	+0.44 V vs SHE	

[a] Cu content was estimated using Bcs as a chromophoric ligand for Cu^{I} in the presence of Gu-HCl (6 M) and dithionite (250 μM); CueO content was estimated from the absorbance at 610 nm using $\epsilon_{610} = 5000$ M^{-1} cm^{-1}. [b] Estimated from a relationship between phenol oxidase activity (substrate, DMP) and the calculated [Cu^{2+}] concentration buffered by BisTris-HCl at pH 7 (Figure 4b inset). [c] Estimated from curve-fitting of the experimental data in Figure 6a,b. [d] Calculated from the Nernst equation with $E^{\circ}_{1/2} = 0.153$ V and the estimated affinities for Cu^{I} and Cu^{II}. [e] From ref 29.

appears to incorporate five copper atoms at identified sites T1, T2, T3, and T4 and is designated here as Cu^{II}-CueO. The extra equivalent found experimentally may be bound at a weaker metal-binding site(s) due to the weak Cu^{II} affinity of the Mops buffer employed here. An X-ray structure of a crystal soaked in sodium acetate (NaAc) buffer containing excess Cu^{2+} detected a weak sixth binding site on the protein surface remote from T1, but this site is unlikely to be functionally important.[7]

The new chromophore detected in the inset of Figure 2 would appear to be characteristic of the T4 center [$Cu^{II}Met_2Asp_2(OH_2)$], identified by X-ray crystallography.[7] Earlier work showed that titration of Cu^{2+} into a CueO solution in Tris-HCl buffer increased the absorbance around 330 and 700 nm, while the absorbance around 600 nm remained essentially unchanged.[11] Previous CueO samples reported absorbance ratios A_{330}/A_{610} between those characteristic of □-CueO and Cu^{II}-CueO (Table 1) and would appear to be mixtures of these two forms.[8,11,12,16] Unless otherwise specified, CueO enzyme employed for all activity assays in this work was Cu^{II}-CueO activated and isolated in Mops buffer.

Phenol Oxidase Activity. Correlated Effects of Buffer and Cu^{2+}. Oxidation of model substrate DMP may be followed by monitoring oxygen consumption with an oxygen sensor electrode. However, it is more convenient and reliable to monitor the absorbance increase at 469 nm which reports formation of the brown oxidation product 3,5,3′,5′-tetramethoxydiphenoquinone (TMPQ; see Experimental Section). The highest activity was achieved with Cu^{II}-CueO in Mops buffer without additional Cu^{2+}. The reaction followed classic Michaelis−Menten kinetics with $K_m = 4.6(3)$ mM and $k_{cat} = 253(6)$ min^{-1} at pH 7.0 (Figure 3; Table 2).

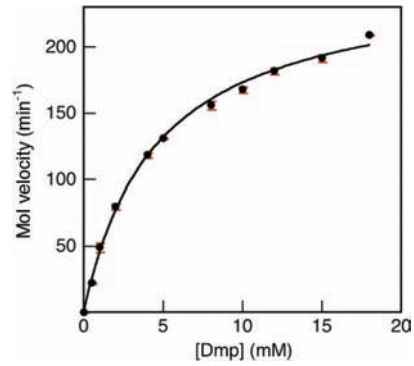

Figure 3. DMP oxidase activity of Cu^{II}-CueO enzyme in air-saturated Mops buffer (50 mM, pH 7) in the absence of added Cu^{2+}. Each data point represents the average of 3−4 independent reactions, with error bars indicating average deviations. The molecular velocity (v/[CueO]$_{total}$) data were fitted directly to the Michaelis−Menten equation to generate the trace shown and the kinetic constants given in Table 2.

However, this activity was inhibited upon addition of a variety of other buffers (20 mM, pH 7) to the assay solution containing Mops buffer (50 mM, pH 7). The observed activity decreased in the following order (Figures 4a (green bars) and S2; buffer $K_D(Cu^{II})$ in M given in parentheses where known):[17,18]

$$\text{Mops} > \text{NaAc}\ (10^{-1.8}) > \text{Tris-HCl}\ (10^{-3.2}) \gg \text{BisTris-HCl}\ (10^{-5.1}) \sim \text{KPi} \quad (1)$$

Buffers NaAc, Tris-HCl, and KPi suppressed the activity. They were employed in previous work, which reported varying activities.[4,8,10−12] It proved necessary to add Cu^{2+} (1−500 μM) in these buffers to activate the preparations, but the amount depended on buffer composition and concentration (e.g., red bars in Figure 4a). Such effects were not observed here for Mops buffer. In fact, the DMP oxidase activity was *suppressed* by the presence of added Cu_{aq}^{2+}, with $IC_{50} \approx 4$ μM (Figure S3, Supporting Information).

The order of DMP oxidase activity in eq 1 correlates inversely with increasing Cu^{II} affinity of the reaction buffers or their precipitating capability. Both Mops and NaAc ($K_D = 10^{-1.8}$ M) have low affinities for Cu^{2+} but, at pH 7, both Tris ($K_D = 10^{-3.2}$ M) and BisTris ($K_D = 10^{-5.1}$ M) exhibit modest affinities.[17,18] Their molar concentrations relative to that of the enzyme (~10^5:1) appear sufficient to strip Cu^{II} from site T4 (see calculations in the inset of Figure 4a). Similarly, KPi buffer precipitates Cu^{2+} efficiently as insoluble $Cu_3(PO_4)_2$ ($K_{sp} = 1.4 \times 10^{-37}$) and so limits free Cu^{2+} to sub-nanomolar concentrations at [KPi] = 20 mM.[19] Cu^{II}-CueO appears to be the active resting form for DMP oxidation; □-CueO is inactive.

(16) Kataoka, K.; Sugiyama, R.; Hirota, S.; Inoue, M.; Urata, K.; Minagawa, Y.; Seo, D.; Sakurai, T. *J. Biol. Chem.* **2009**, *284*, 14405–14413.
(17) Scheller, K. H.; Abel, T. H. J.; Polanyi, P. E.; Wenk, P. K.; Fischer, B. E.; Sigel, H. *Eur. J. Biochem.* **1980**, *107*, 455–466.
(18) Martell, A. E.; Smith, R. M.; Motekaitis, R. J. NIST Critically Selected Stability Constants of Metal Complexes, Version 8.0; NIST Standard Reference Database 46; U.S. Department of Commerce, NIST Program: Gaithersburg, MD, 2004; http://www.nist.gov/srd/nist46.htm.
(19) Lide, D. R. *CRC Handbook of Chemistry and Physics*, 84th ed.; CRC Press: Boca Raton, FL, 2004.

Table 2. Kinetic Constants for Steady-State Turnover of DMP and $[Cu^{I}(Bca)_2]^{3-}$ by CueO in Buffer (50 mM, pH 7)[a]

expt	buffer	k_1 (μM^{-1} min^{-1})	k_{-1} ($\times 10^{-3}$ μM^{-2} min^{-1})	k_{-1}/k_1 (μM^{-1})	K_m (mM)	k_{cat} ($\times 10^2$ min^{-1})	k_{cat}/K_m (M^{-1} min^{-1})
			DMP Substrate				
Figure 3	Mops				4.6	253	0.055
	BisTris				~0	~0	
			$[Cu^{I}(Bca)_2]^{3-}$ Substrate				
	Mops	~0	~0		~0	~0	
Figure 6a	BisTris	0.38	6.0	0.016	0.24[b]	6.9	2.9
Figure 6b(i)	BisTris	0.35	7.4	0.021	0.17[b]	5.0	2.9
Figure 6b(ii)	BisTris	0.47	10	0.022	0.24[b]	5.2	2.2

[a] The kinetic data were obtained by direct curve-fittings of the experimental data in Figure 3 to the Michaelis−Menten equation for DMP oxidase activity and of the data in Figure 8 to eq 7 for cuprous oxidase activity on substrate $[Cu^{I}(Bca)_2]^{3-}$; [b] K_m in eq 7 may be defined by $(k_2 + k_{-1}[Bca]^2)/k_1$ and is dependent on the free ligand concentration [Bca]. Since k_2 ($= k_{cat}$) $\gg k_{-1}[Bca]^2$ when free ligand concentration is low, such as [Bca] <20 μM, the second term $k_{-1}[Bca]^2$ may be ignored under this condition and the K_m calculated by (k_{cat}/k_1).

Copper centers T1, T2, and T3 exhibit high binding affinities and do not dissociate readily.[20] The T1 center is usually responsible for substrate oxidation but, in CueO, is buried under the Met-rich α-helix (Figure 1a). It is apparent that communication with organic substrate molecules requires the extra copper center T4 to serve as an electron-transfer mediator, as depicted in Scheme 1. Mutation of residues contributing to this T4 site resulted in loss of DMP oxidase activity *in vitro* and of copper tolerance *in vivo*, confirming its essential role for enzyme function.[7]

Addition of Cu_{aq}^{2+} into the pH buffers listed on the right-hand side of eq 1 effectively creates metal buffers controlling Cu^{2+} availability and allowing partial or full occupation of the T4 site (e.g., eq 2).

$$\square\text{-CueO} + Cu^{II}\text{-BisTris} \rightleftharpoons Cu^{II}\text{-CueO} + \text{BisTris} \qquad (2)$$

A linear correlation was found between the free Cu^{2+} concentration buffered by BisTris (50 mM, pH 7) and the DMP oxidase activity of CueO (inset, Figure 4a). This relationship allowed estimation of the Cu^{II} binding affinity of T4 via the known affinity of BisTris:[17] $K_D = 5.5 \times 10^{-9}$ M (Table 1; see Experimental Section). Knowledge of this affinity permits a quantitative interpretation of the relationships between DMP oxidase activity, buffer composition, and Cu^{2+} availability observed in Figure 4a. In particular, in Mops buffer (low affinity for Cu^{2+}), the T4 site remains occupied and the enzyme Cu^{II}-CueO exhibits full DMP oxidase activity without the need for added Cu^{2+}, even at the enzyme concentrations $10^{-6}-10^{-7}$ M employed routinely in the assay (see Experimental Section). In contrast, in this buffer, excess added Cu^{2+} suppresses DMP oxidation sensitively ($IC_{50} \approx 4$ μM; Figure S3). The mechanism for the inhibition remains unknown but may be due to more than one Cu^{II} ion binding in the vicinity of T4, thereby altering its reduction potential and disrupting electron transfer from substrate to the T1 center.

Addition of heavy metal ions such as Ag^+ or Hg^{2+} destroyed enzyme activity completely and irreversibly (Figure S2(iv), Supporting Information). The electronic spectra of such solutions were essentially identical to that of □-CueO with its intact T1, T2, and T3 centers (Figure 2a). It appears that these metal ions bind at T4 with high affinity (see below) and block the electron transfer between substrate and the T1 center. Addition of high-affinity Cu^{II} ligands such as Edta to Cu^{II}-CueO also arrested the enzyme activity completely (Figure S2(iv)). However, subsequent addition of excess Cu^{2+} recovered the activity.

In summary, the phenol oxidase activity of CueO relies on occupation of a single Cu^{II} ion at the labile T4 site. Consequently, the activity is sensitive to the reaction medium and is optimized within a narrow range of available labile Cu_{aq}^{2+} concentrations ($10^{-6}-10^{-9}$ M under typical assay conditions; Figures 4a, S2, and S3). It is unlikely that the concentration of available Cu_{aq}^{2+} in the periplasmic space is maintained within this range. Some periplasmic *E. coli* proteins such as PcoC bind Cu^{II} with sub-picomolar affinities.[21] In the presence of these proteins, CueO would lose phenol oxidase activity completely. Indeed, addition of a trace amount of *apo*-PcoC into the reaction medium in Mops buffer led to complete loss of the phenol oxidase activity (Figure S2(iv)). Therefore, CueO is unlikely to function as a phenol oxidase *in vivo*.

Cuprous Oxidase Activity. Correlated Effects of Buffer and Cu^{2+}. CueO has also been proposed to be a cuprous oxidase, detoxifying Cu^{I} pumped from the cytoplasm by the P-type ATPase CopA as a response to elevated levels of environmental copper under aerobic conditions.[1] This suggestion is based upon oxidation of the complex $[Cu^{I}(MeCN)_4]^+$ stabilized by a low percentage of MeCN in the buffer.[13] Lack of a convenient spectroscopic probe for either $[Cu^{I}(MeCN)_4]^+$ or Cu_{aq}^{2+} meant that the reaction must be followed by a dioxygen sensor, but in our hands, the technique was unable to distinguish adequately between direct and CueO-catalyzed oxidation of this complex by O_2 (Figure 5a). It is apparent that $[Cu^{I}(MeCN)_4]^+$ is too labile under the conditions to act as a biologically relevant model substrate or to allow extraction of meaningful kinetic data (Figure 5a, inset).

In the search for better model cuprous substrates for reliable study, the purple complex anion $[Cu^{I}(Bca)_2]^{3-}$ (Figure 5b, inset; $\lambda_{max} = 562$ nm, $\epsilon = 7900$ M^{-1} cm^{-1}, $\beta_2 = 10^{17.2}$ M^{-2})[22,23] was found to satisfy the requirements of a robust chromophoric model substrate, equivalent to the use of DMP as a probe of phenol oxidase activity. Excess Bca reacts with Cu^+ quantitatively to produce the stable anion $[Cu^{I}(Bca)_2]^{3-}$ with "free" Cu^+ concentrations being buffered around the sub-picomolar level,[24] a concentration range accessible by many periplasmic Cu^{I}-

(20) Galli, I.; Musci, G.; Bonaccorsi di Patti, M. C. *J. Biol. Inorg. Chem.* **2004**, *9*, 90–95.

(21) Djoko, K. Y.; Xiao, Z.; Huffman, D. L.; Wedd, A. G. *Inorg. Chem.* **2007**, *46*, 4560–4568.

(22) Xiao, Z.; Donnelly, P. S.; Zimmermann, M.; Wedd, A. G. *Inorg. Chem.* **2008**, *47*, 4338–4347.

(23) A smaller $\beta_2 = 4.6 \times 10^{14}$ M^{-2} for $[Cu^{I}(Bca)_2]^{3-}$ was estimated independently by isothermal titration calorimetry: Yatsunyk, L. A.; Rosenzweig, A. C. *J. Biol. Chem.* **2007**, *282*, 8622–8631. In that work, the Cu^+ solution was generated by reduction of Cu^{2+} with ascorbate in 200 mM NaCl, which stabilizes Cu^+ as $[Cu^{I}Cl_4]^{3-}$ and related chloro complexes. Titration with Bca would involve a conversion of species such as $[Cu^{I}Cl_4]^{3-}$ (rather than Cu^{+}_{aq}) to $[Cu^{I}(Bca)_2]^{3-}$, diminishing the observed heat release.

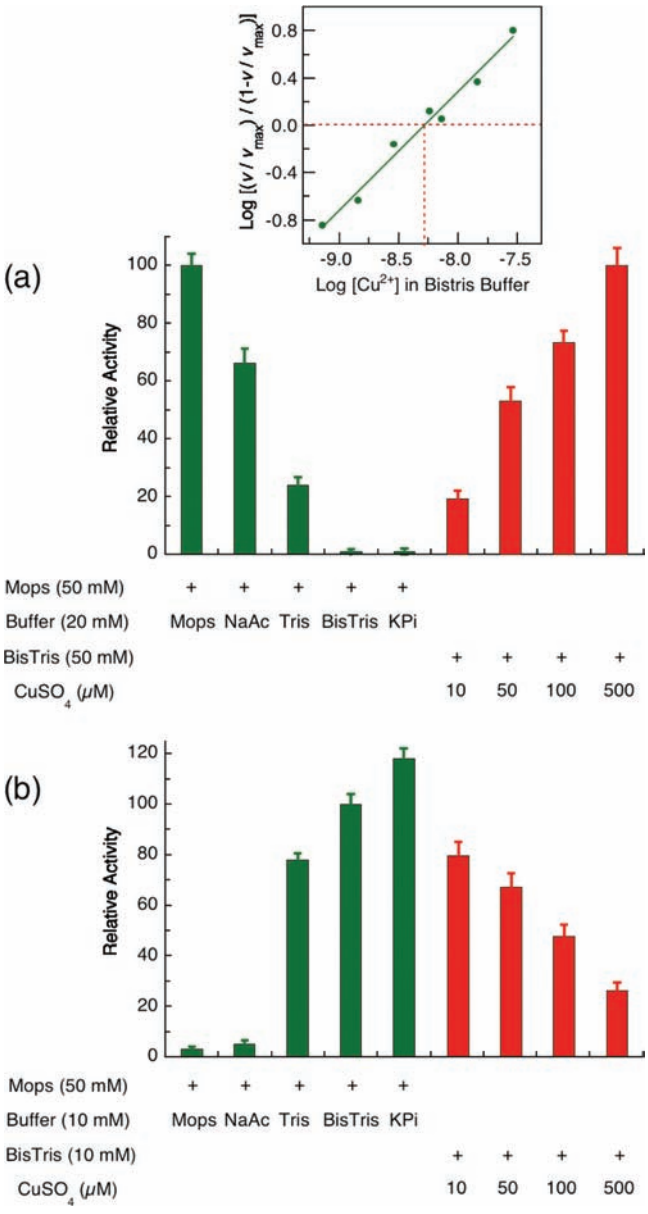

Figure 4. Correlated effects of buffer composition (green bars) and Cu^{2+} concentration (red bars) on the oxidase activities of CueO at pH 7.0: (a) with substrate DMP (10 mM; activity normalized relative to that in Mops buffer) [Inset: estimation of $K_D(Cu^{II})$ of the T4 site from the variation of DMP oxidase activity in BisTris-HCl buffer upon addition of Cu^{2+} (see Experimental Section for details)] and (b) with substrate $[Cu^{I}(Bca)_2]^{3-}$ (100 μM; prepared by mixing Cu^{+} and Bca^{2+} in 1:2.5 molar ratio; activity normalized relative to that in BisTris buffer). Each data point represents the average of at least three runs, with error bars indicating average deviations.

binding proteins.[21,22,25−27] In addition, $[Cu^{I}(Bca)_2]^{3-}$ resists air oxidation in common biological buffers, including Cu^{II}-binding buffers such as BisTris-HCl (Figure 5b(i)), but is oxidized readily with CueO as a catalyst (Figure 5b(ii)). The associated bleaching of the solution allows the cuprous oxidase reaction to be followed conveniently (Figure S4, Supporting Information). These advantages allow, for the first time, a reliable and quantitative investigation of both the thermodynamics and the kinetics of CueO acting as a cuprous oxidase.

The cuprous oxidase activities of CueO correlated with buffer composition and the availability of Cu^{2+}. However, the effects were diametrically opposite to those observed for DMP oxidase

Scheme 1. Model of the Reaction of CueO as a DMP Oxidase[a]

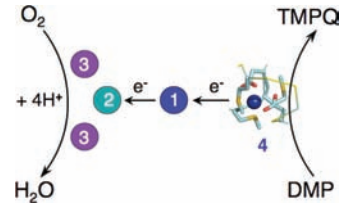

[a] The resting state of the enzyme features a Cu^{II} ion (in blue sphere) bound in site T4 (proposed ligands shown as sticks) which acts as an electron-transfer mediator between site T1 and substrate DMP. Loss of labile T4 Cu^{II} renders the enzyme inactive as a phenol oxidase.

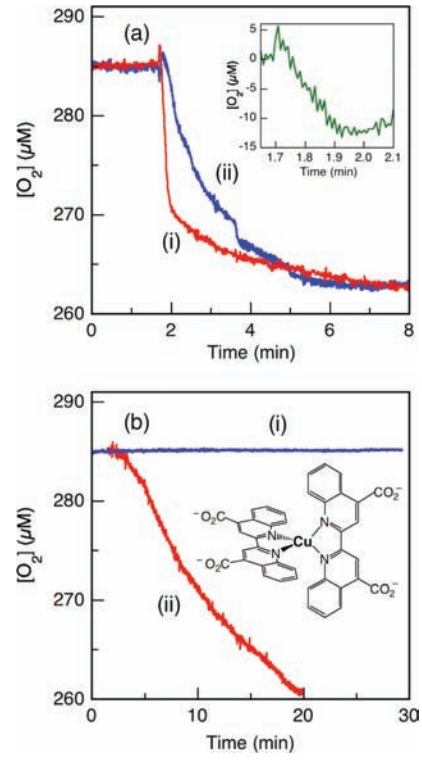

Figure 5. O_2 consumption rate as monitored by a Clark-type oxygen electrode. (a) Upon addition of $[Cu^{I}(MeCN)_4]^{+}$ (100 μM) at $t = 2$ min: (i) into air-saturated Mops buffer (50 mM, pH 7) containing MeCN (~10%) and CueO (0.25 μM) and (ii) into the same buffer solution but without enzyme. Inset: difference in O_2 consumption rate between (i) and control (ii). (b) (i) A solution of $[Cu^{I}(Bca)_2]^{3-}$ (200 μM) in air-saturated Tris-HCl buffer (50 mM, pH 7) and (ii) upon addition of CueO (1.0 μM) at $t = 2$ min into the solution of (i). Inset: structure of $[Cu^{I}(Bca)_2]^{3-}$.

activity (Figure 4b vs 4a). Weak cuprous oxidase activity was observed only in Mops and NaAc buffers, and the high activity in BisTris buffer was suppressed by addition of Cu^{2+} (Figure 4b). These results suggest that the resting state of the cuprous oxidase form is □-CueO, not Cu^{II}-CueO. This implies that site T4 must be vacant and be available for Cu^{I} docking and oxidation.

Excess free Bca ligand is present in the reaction solutions to ensure all Cu^{I} is present as substrate $[Cu^{I}(Bca)_2]^{3-}$. However, this did not promote cuprous oxidase activity in buffers NaAc and Mops which have low affinities for Cu^{2+} (Figure 4b), consistent with ligand Bca also having a low affinity for Cu^{2+} and being unable to remove product Cu^{II} from the T4 site (see below and Figure 8). Addition of Ag^{+} (4 equiv) into the reaction medium inhibited the cuprous oxidase activity completely, presumably because this cation occupied the T4 site irreversibly.

Steady-State Kinetics. A concentrated stock solution of $[Cu^{I}(Bca)_2]^{3-}$ of molar ratio Bca:Cu^{I} = 2.50 was prepared in Mops buffer (10 mM, pH 7), imposing an initial condition of $[Bca]_{free} = 0.5[Cu^{I}(Bca)_2{}^{3-}]$ with negligible contribution from the 1:1 complex $[Cu^{I}(Bca)]^{-}$. This solution was diluted sequentially into air-saturated BisTris-HCl buffer (50 mM, pH 7) to prepare a series of substrate solutions of different concentrations. Catalysis of the oxidation of $[Cu^{I}(Bca)_2]^{3-}$ was initiated by introduction of Cu^{II}-CueO (0.1 μM), which was rapidly converted to □-CueO upon mixing with the BisTris-HCl buffer. The oxidation rate was followed by the change in absorbance at 562 nm (Figures S4 and S5, Supporting Information).

Oxidation of each equivalent of $[Cu^{I}(Bca)_2]^{3-}$ releases 2 equiv of free Bca ligand into solution, and this may affect the oxidation rate. To obtain a known relationship between $[Bca]_{free}$ and $[Cu^{I}(Bca)_2{}^{3-}]$ for quantitative kinetic analysis, the oxidation rates v were recorded when the reaction was only 10% complete. At this point, $[Bca]_{free} = 0.8[Cu^{I}(Bca)_2{}^{3-}]$ (see Experimental Section for details). With increase in [Cu^{I}:2.8Bca], molecular velocities $v_{measured}/[CueO]_{total}$ increased initially, reached a maximum, and then decayed slowly (Figure 6a). These observations are consistent with the cuprous substrate being the complex anion $[Cu^{I}(Bca)_2]^{3-}$ and not dissociated "free" Cu^{+} ion because, under the constraint of $[Bca]_{free} = 0.8[Cu^{I}(Bca)_2{}^{3-}]$, an increase in $[Cu^{I}]$ leads to an increase in both $[Cu^{I}(Bca)_2{}^{3-}]$ and $[Bca]_{free}$ but a decrease in $[Cu^{+}]_{free}$ due to the effect of increasing $[Bca]_{free}$ (see Figure 6c).

The experimental data in Figure 6a could not, however, be fitted to the classical Michaelis−Menten equation (red trace). This is apparently due to the opposing effects of the concentrations of $[Cu^{I}(Bca)_2]^{3-}$ and Bca on the Cu^{I} oxidation rate. An increase in the former accelerates the oxidation, while an increase in the latter limits Cu^{I} availability (Figure 6c), suppressing the reaction. Indeed, when the substrate concentration of $[Cu^{I}(Bca)_2]^{3-}$ was kept constant, the Cu^{I} oxidation rate decreased with increasing Bca concentration (Figure 6b). Consequently, the kinetic analysis was modified to include these different contributions.

Analysis of Steady-State Kinetics. A general scheme of catalytic conversion of metal substrate M^{I}-L_n to product M^{II}-L'_x by metallo-enzyme E may be depicted by eqs 3a and 3b:

$$M^{I}\text{-}L_n + E \underset{k_{-1}}{\overset{k_1}{\rightleftharpoons}} E\text{-}M^{I}\text{-}L_m + (n - m)L \qquad (3a)$$

$$E\text{-}M^{I}\text{-}L_m + xL' \xrightarrow{k_2} E + M^{II}\text{-}L'_x + mL \qquad (3b)$$

For the present case, E = T4 site of CueO; L = Bca; M^{I}-L_n = $[Cu^{I}(Bca)_2]^{3-}$; L′ = BisTris; and M^{II}-L'_x = $[Cu^{II}$-BisTris$]_{aq}$. The mechanism implies transfer of Cu^{I} from $[Cu^{I}(Bca)_2]^{3-}$ to the site T4, followed by electron transfer to site T1 and trapping of product Cu^{2+} by buffer ligand which is present in excess. The enzyme−substrate complex E-M^{I}-L_m = CueO-Cu^{I}-$(Bca)_m$ that can be oxidized may be binary or ternary (m = 0, 1, or 2). Parameters k_1 and k_{-1} are the overall rate constants for, respectively, the forward and reverse reactions of eq 3a, and k_2 is the overall rate constant of eq 3b for irreversible conversion of the enzyme−substrate complex E-M^{I}-L_m ($m \le n$) to product M^{II}-L'_x.

Under catalytic (excess substrate) and steady-state ([E-M^{I}-L_m] constant) conditions, the overall reaction rate v is limited by the rate of conversion of the complex E-M^{I}-L_m to M^{II}-L'_x and E (eqs 4 and 5):

$$v = k_2[E\text{-}M^{I}\text{-}L_m] \qquad (4)$$

$$k_1[M^{I}\text{-}L_n][E] = k_{-1}[E\text{-}M^{I}\text{-}L_m][L]^{(n-m)} + k_2[E\text{-}M^{I}\text{-}L_m] \qquad (5)$$

$$[E] = [E]_{total} - [E\text{-}M^{I}\text{-}L_m] \qquad (6)$$

Combination of eqs 4, 5 and 6 gives an extended Michaelis−Menten equation (eq 7):

$$v = \frac{V_{max}[M^{I}\text{-}L_n]}{k_2/k_1 + (k_{-1}/k_1)[L]^{(n-m)} + [M^{I}\text{-}L_n]} \qquad (7)$$

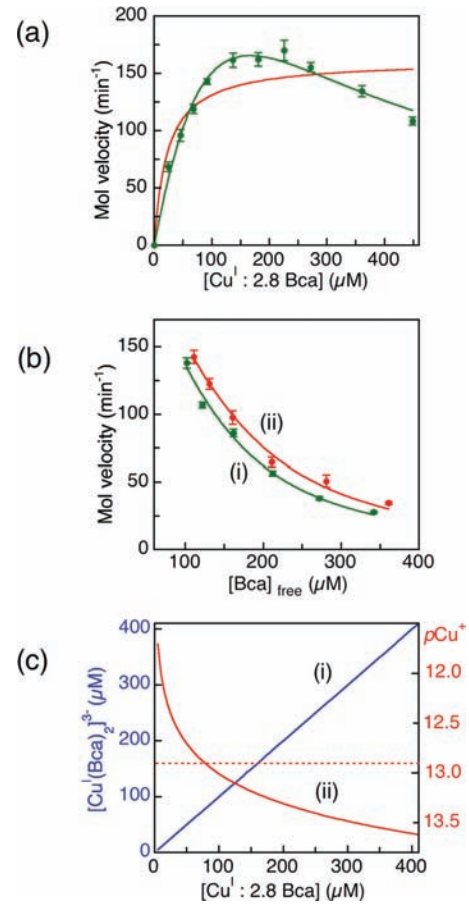

Figure 6. Oxidation of substrate $[Cu^{I}(Bca)_2]^{3-}$ by CueO (0.1 μM) in air-saturated BisTris-HCl buffer (50 mM, pH 7.0). (a) The substrate was prepared by mixing $[Cu^{I}(MeCN)_4]^{+}$ and Bca^{2-} in a fixed molar ratio of 1:2.5, but the reaction rate was determined at ~90% of initial $[Cu^{I}(Bca)_2]^{3-}$ concentration, thus $[Bca]_{free} = 0.8[Cu^{I}(Bca)_2{}^{3-}]$. (b) $[Cu^{I}(Bca)_2]^{3-}$ was fixed at a constant concentration of 144 (green) or 195 μM (red) at points where the reaction rates were measured. (c) Change in $[Cu^{I}(Bca)_2]^{3-}$ and $[Cu^{+}]$ concentrations with increasing concentrations of [Cu^{I}:2.8Bca]. The formation constant $\beta_2 = 10^{-17.2}$ M^{-2} for $[Cu^{I}(Bca)_2]^{3-}$ was used to calculate $[Cu^{+}]$. $K_D(Cu^{I})$ for site T4 in CueO is indicated by the red dashed line. Each data point in (a) and (b) represents the average of 3−4 independent reactions, with error bars indicating average deviations. The molecular velocity data ($v/[CueO]_{total}$) were fitted directly to eq 7, with details given in the Experimental Section, generating the traces shown and the kinetic data given in Table 2. The red trace in (a) was the fitting of the same data to the Michaelis−Menten equation.

where $V_{max} = k_2[E]_{total}$ is the maximum reaction rate under the assumption that $[M^I\text{-}L_n] \gg [E]$ and that all enzyme molecules have substrate bound.

Note that when $m = n$, eq 7 becomes the classic Michaelis−Menten equation: $\upsilon = V_{max}[S]/(K_M + [S])$, where $K_M = (k_2 + k_{-1})/k_1$ and [S] is substrate concentration. This corresponds to two possible situations: (i) ternary complex E-M^I-L_n converts to product M^{II} directly without dissociation of carrier ligand L or (ii) M^I-L_n dissociates completely before transfer of M^I ion to the enzyme. However, when $m < n$, the term K_M in the Michaelis−Menten equation becomes dependent on the ligand concentration [L] raised to the power $(m - n)$ and is split into two terms, k_2/k_1 and $(k_{-1}/k_1)[L]^{(n-m)}$. When the reaction rate is expressed in terms of molecular velocity ($\upsilon/[E]_{total}$ in units of time^{-1}), the term k_2 becomes k_{cat}, which may be obtained from V_{max} together with k_1 and k_{-1} as well.

In the present system, attempts were made to apply eq 7 to the experimental data of Figure 6. There are two variables ([Bca] and $[Cu^I(Bca)_2^{3-}]$) and four parameters (k_1, k_{-1}, k_2 (or k_{cat}), and $(n - m)$). To simplify analysis, the two sets of data in Figure 6b were fitted first to eq 7 for reaction points where the initial substrate concentrations $[Cu^I(Bca)_2^{3-}]$ (150 and 200 μM) had diminished to respective fixed values (144 and 195 μM). Rates were calculated as a function of varying ligand concentration, [L] = [Bca], which was the sum of initial $[Bca]_{free}$ and [Bca] released from the initial substrate oxidation. This allowed a reliable definition of the parameter $(n - m)$, which is related to [Bca] only. The fittings gave $(n - m) = 1.8$ and 1.9, respectively, for the data sets (i) and (ii) of Figure 6b. Subsequently, eq 7 with $(n - m) = 2$ was used to fit the three sets of data in Figure 6a,b without further restriction but including the influence of Bca ligand released into solution upon oxidation of $[Cu^I(Bca)_2]^{3-}$ (see Experimental Section for details). Each of the three sets of experimental data was fitted satisfactorily with correlation coefficients $R \geq 0.99$ (Figure 6). The derived kinetic parameters are consistent even though the experimental conditions varied significantly (Table 2). Note that the effect of product Cu^{2+} (Figure 4b, red bars) was not considered in the kinetic analysis. At early stages of the reaction, the concentration of Cu^{II} product is low. In addition, the presence of a high concentration of BisTris buffer (50 mM, $K_D = 10^{-5.1}$ M) ensures that a low concentration of Cu^{2+} (<100 μM) has a negligible effect on the oxidation rate (Figure S5).

Analysis of the Reaction Mechanism. The parameter $(n - m)$ is the number of carrier ligands L = Bca released upon binding of metal substrate $M^I = Cu^I$ to enzyme E (eq 3a). Its estimated value of ~2 is significant in two aspects: (i) it consolidates the previous conclusion that the cuprous substrate is the intact anion $[Cu^I(Bca)_2]^{3-}$, not "free" Cu, and (ii) it means that the only enzyme−substrate complex which may be oxidized directly to product Cu^{II} is Cu^I−CueO, i.e., both Bca ligands must be dissociated prior to the oxidation of Cu^I.

Scheme 2 presents a model for the oxidation of Cu^I carried by $[Cu^I(Bca)_2]^{3-}$ catalyzed by the enzyme □-CueO in Cu^{II} binding buffers such as in BisTris. The resting-state □-CueO (represented by structure i)[7] provides a site for docking of $[Cu^I(Bca)_2]^{3-}$ and formation of transient ternary complex(es) (structure ii). Dissociation of the two Bca ligands and insertion of Cu^I (red sphere) into T4 leads to structure iii and electron transfer to the T1 site. The resultant Cu^{II} center (blue sphere, structure iv) is labile, and product Cu^{II} is trapped by buffer BisTris (present in a large excess; $K_D(Cu^{II}) = 10^{-5.1}$ M), returning the system to the active resting form.

Scheme 2. Proposed Mechanism for the Reaction of CueO as a Cuprous Oxidase Acting upon Model Substrate $[Cu^I(Bca)_2]^{3-}$ in BisTris Buffer[a]

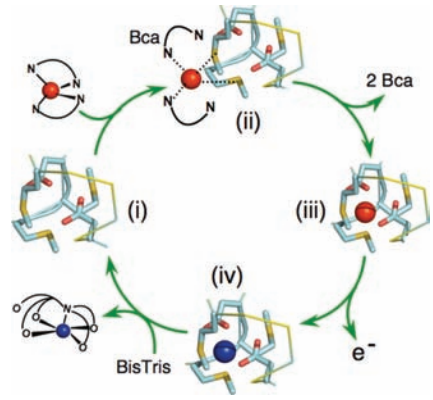

[a] Cu^I, red sphere; Cu^{II}, blue sphere. The resting state features an empty T4 site (i), which acts as the docking site for Cu^I binding (ii, iii) and oxidation (iv). The product Cu^{II} is removed and trapped by buffer ligand BisTris in this representation.

The model predicts that catalytic efficiency is enhanced by increasing substrate concentration $[Cu^I(Bca)_2^{3-}]$ but is inhibited by increasing free carrier ligand concentration [Bca] (Figure 6). Excess Bca suppresses the migration of Cu^I from $[Cu^I(Bca)_2]^{3-}$ to T4. Under the conditions in which the molar ratio Bca:Cu^I was set at 2.8 (Figure 6a), an increase of Cu^I_{total} led to an increase in both $[Cu^I(Bca)_2^{3-}]$ and [Bca]. The effect of the former dominated the catalytic rate at low substrate concentrations, but the effect of the latter dominated the rate at high substrate concentrations when the site T4 approaches saturation. Hence, under the conditions, the oxidation rate increased initially, reached a maximum, and then decreased (Figure 6a). On the other hand, the oxidation rate was suppressed by buffers with low affinity for Cu^{II} (Mops and NaAc) or by addition of excess Cu^{2+} into the reaction medium (Figure 4b). Both inhibit the last step of the cycle, in which Cu^{II} is removed from the T4 site (eq 3b).

Thermodynamics of Site T4. The affinity of the T4 site for Cu^I may be estimated from the derived kinetic parameter (k_{-1}/k_1) estimated from eq 7. This parameter is, in fact, the inverse of the equilibrium constant K_{ex} of the following Cu^I exchange reaction, rewritten from general eq 3a for the present system:

$$\square\text{-CueO} + [Cu^I(Bca)_2]^{3-} \rightleftharpoons Cu^I\text{-CueO} + 2Bca^{2-} \quad (8)$$

$$K_{ex} = \frac{[Cu^I\text{-CueO}][Bca]^2}{[\square\text{-CueO}][Cu^I(Bca)_2]}$$

$$\text{i.e.,} \quad k_{-1}/k_1 = (K_{ex})^{-1} = K_D\beta_2 \quad (9)$$

where K_D and β_2 are, respectively, the Cu^I dissociation constant of the T4 site in CueO and the accumulated formation constant of the anion $[Cu^I(Bca)_2]^{3-}$. Consequently, K_D is calculated to be 1.3×10^{-13} M from the reported β_2 value for $[Cu^I(Bca)_2]^{3-}$ anion[22] and the estimates of (k_{-1}/k_1) listed in Table 2.

This affinity is supported by the competition observed between Cu^{II}-PcoC and □-CueO for Ag^I, the redox-inactive congener of Cu^I (Figure 7). Cu^{II}-PcoC is a Cu^I binding protein from *E. coli* with affinity estimated to be 2×10^{-13} M,[21,25] similar to that estimated above for □-CueO. Each protein binds Ag^I at its Cu^I site to produce the stable forms, Ag^ICu^{II}-PcoC and Ag^I-CueO. The former protein elutes as a single peak from

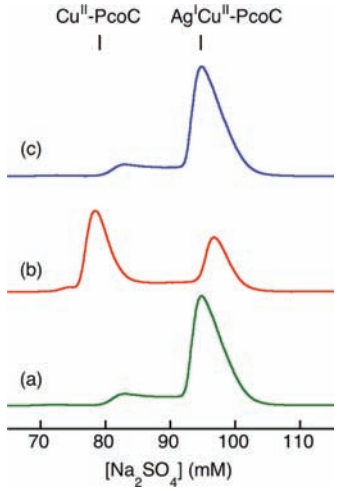

Figure 7. Exchange of Ag^I between Ag^ICu^{II}-PcoC and □-CueO in Mops buffer (50 mM, pH 7.0). Reaction mixtures (25 μM in each protein) were applied to a Mono-S HR 5/5 cation-exchange column. (a) Ag^ICu^{II}-PcoC only; (b) equimolar mixture of Ag^ICu^{II}-PcoC and □-CueO; (c) as for (b) but with $CuCl_2$ (50 μM) premixed with □-CueO. Ag^ICu^{II}−PcoC and Cu^{II}−PcoC eluted at different salt concentrations (markers), while CueO was separated in the column flow-through. The increased absorbance starting at the elution position of Cu^{II}−PcoC is due to slow decomposition of Ag^ICu^{II}-PcoC induced by the affinity of the Mono-S resin for Ag^+ ions.

an analytical cation-exchange column (Figure 7a) while CueO elutes in the column flow-through. A solution containing equimolar Ag^ICu^{II}-PcoC and □-CueO in Mops buffer (20 mM, pH 7) was incubated for 30 min and then applied to the cation-exchange column for analysis. About 60% of Ag^ICu^{II}-PcoC was converted to Cu^{II}-PcoC according to eq 10 (Figure 7b), consistent with similar affinities of both proteins for Ag^I (and thus likely for Cu^I as well):

$$\square\text{-CueO} + Ag^ICu^{II}\text{-PcoC} \rightleftharpoons Ag^I\text{-CueO} + \square Cu^{II}\text{-PcoC} \quad (10)$$

$$Cu^{II}\text{-CueO} + Ag^ICu^{II}\text{-PcoC} \not\rightarrow Ag^I\text{-CueO} + \square Cu^{II}\text{-PcoC} + Cu^{2+} \quad (11)$$

On the other hand, in Mops buffer, Cu^{2+} can also occupy the T4 site in CueO, but not the Cu^I site in Cu^{II}-PcoC. Addition of excess of Cu^{2+} into the above reaction solution prevented migration of Ag^I from PcoC to CueO (eq 11; Figure 7c).

The estimated affinity of site T4 for Cu^I is higher than that for Cu^{II} (Table 1). This result is supported by the observation that the phenol oxidase activity arrested by Ag^+ cannot be restored by addition of Cu^{2+} (*vide supra*; note the difference between eqs 11 and 12):

$$Ag^I\text{-CueO} + Cu^{2+} \not\rightarrow Cu^{II}\text{-CueO} + Ag^+ \quad (12)$$

An X-ray crystal structure modeled the Cu^{II} center bound at the T4 site as $Cu^{II}(Met)_2(Asp)_2(H_2O)$ (Figure 1b).[7] While a mixture of hard and soft ligands is consistent with the relatively weak binding affinity determined here for Cu^{II} ($K_D = 5.5 \times 10^{-9}$ M), it is inconsistent with the high affinity for Cu^I ($K_D = 1.3 \times 10^{-13}$ M). Notably, in the crystal structure, uncoordinated M440 is located on the same binding loop as ligands D439 and M441. A minor translation of this binding loop is all that is required to switch metal binding ligands from D439 to M440 while maintaining M441 as a Cu^I ligand. This would lead to a

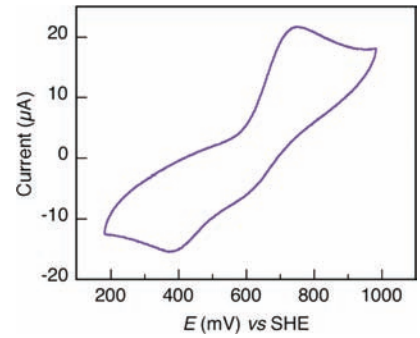

Figure 8. Cyclic voltammogram of $[Cu^I(Bca)_2]^{3-}$ (1.0 mM) in KPi buffer (20 mM, pH 7.0; NaCl, 100 mM) at a scan rate of 20 mV s^{-1}.

$Cu^I(Met)_3L_n$ site related to those seen in a number of periplasmic Cu^I binding proteins.[28]

The estimates of K_D for binding of both Cu^I and Cu^{II} at the T4 site permit the Nernst equation to provide a value of 0.42 V vs SHE for the reduction potential of the Cu^{II}/Cu^I couple at site T4. This value is about the same as that of the T1 center (0.44 V vs SHE) determined recently by direct electrochemistry at pH 7.[29] These reduction potentials are positive enough to directly oxidize labile Cu^+ ions such as those provided by $[Cu^I(MeCN)_4]^+$. Consequently, with $[Cu^I(MeCN)_4]^+$ as substrate, oxidation may proceed via a mixed mechanism involving Scheme 2 (inner sphere) and the equivalent of Scheme 1 (outer sphere), plus direct oxidation by air (Figure 5a(ii)). This rationalizes previous observations that excess Cu^{2+} promoted cuprous oxidase activity with $[Cu^I(MeCN)_4]^+$ as substrate.[8,13,14] However, model substrate $[Cu^I(Bca)_2]^{3-}$ is stable in air. Direct electrochemical experiments revealed that the redox couple of $[Cu^I(Bca)_2]^{2-/3-}$ is irreversible, with an oxidation process at ~0.72 V and two reduction processes at ~0.4 and 0.6 V, respectively (Figure 8). On one hand, these data confirm that the reduction potentials of both the T1 or T4 centers (~0.4 V) are too negative to oxidize the intact anion $[Cu^I(Bca)_2]^{3-}$ directly in Mops or NaAc buffers (Figure 4b). On the other hand, these data also suggest that the anion $[Cu^{II}(Bca)_2]^{2-}$ is not stable under the conditions, consistent with the previous conclusion that Bca has a low affinity for Cu^{2+} and is unable to remove product Cu^{II} from the T4 site. Therefore, transfer of Cu^I from the substrate to the ligand set provided by the T4 site enhances the relative Cu^{II} binding affinity and shifts the reduction potential negatively to promote Cu^I oxidation. The process can proceed via Scheme 2 only. Thus, $[Cu^I(Bca)_2]^{3-}$ is a *bona fide* model

(24) The "free" Cu^+ concentration buffered by Bca and Bcs may be calculated by the formula $[Cu^+] = ([Cu^IL_2]/[L]^2)(\beta_2)^{-1}$ and thus is dependent on both concentrations of $[Cu^IL_2]$ and [L]. Assuming that 50% of ligand L binds Cu^I and 50% is free, i.e., $[L] = 2[Cu^IL_2]$, then $[Cu^+] = ([Cu^IL_2]/(2[Cu^IL_2])^2)(\beta_2)^{-1} = (1/4)([Cu^IL_2])^{-1}(\beta_2)^{-1}$. As a metal buffer, $[Cu^IL_2]$ concentrations are usually controlled in the range 10−50 μM, correlating to $[Cu^+]$ concentrations in the range 1.6×10^{-13}−3.2×10^{-14} M for L = Bca and 4.0×10^{-16}−7.9×10^{-17} M for L = Bcs, according to respective β_2 values reported in the literature. In practice, these buffer ranges may be extended further on both ends by variation of the total concentration ratio of $[L]/[Cu^+]$.

(25) Chong, L. X.; Ash, M. R.; Maher, M. J.; Hinds, M. G.; Xiao, Z.; Wedd, A. G. *J. Am. Chem. Soc.* **2009**, *131*, 3549–3564.
(26) Zhang, L.; Koay, M.; Maher, M. J.; Xiao, Z.; Wedd, A. G. *J. Am. Chem. Soc.* **2006**, *128*, 5834–5850.
(27) Xue, Y.; Davis, A. V.; Balakrishnan, G.; Stasser, J. P.; Staehlin, B. M.; Focia, P.; Spiro, T. G.; Penner-Hahn, J. E.; O'Halloran, T. V. *Nat. Chem. Biol.* **2008**, *4*, 107–109.
(28) Davis, A. V.; O'Halloran, T. V. *Nat. Chem. Biol.* **2008**, *4*, 148–151.
(29) Miura, Y.; Tsujimura, S.; Kurose, S.; Kamitaka, Y.; Kataoka, K.; Sakurai, T.; Kano, K. *Fuel Cells* **2009**, *9*, 70–78.

substrate which mimics the properties of the periplasmic Cu^I binding proteins.[24] The conclusion is consistent with that of the kinetic analysis: dissociation of the Bca ligands must occur prior to oxidation (Scheme 2). It also rationalizes the observation that excess Cu^{2+} does not promote legitimate cuprous oxidase activity. In fact, it inhibits it (Figure 4b, red bars).

Thermodynamic versus Kinetic Control of Cu^I Oxidation. Cu^I centers stabilized by proteins or by synthetic ligands possess high reduction potentials and are resistant to aerial oxidation. Transfer of the Cu^I center from the substrate carrier to the T4 site in CueO is the key to the oxidation. The Cu^I insertion is controlled by both kinetic factors and the thermodynamic gradient. A sub-picomolar affinity of T4 in CueO for Cu^I falls within the sensitive buffering range of the ligand Bca for Cu^+ (see red dashed line in Figure 6c). This ensures a favorable thermodynamic gradient for migration of Cu^I from $[Cu^I(Bca)_2]^{3-}$ to T4 in CueO.

In comparison to the classic Michaelis−Menten equation, K_m for eq 7 may be defined by $(k_2 + k_{-1}[Bca]^2)/k_1$ and is dependent on free ligand concentration [Bca]. Since k_2 ($= k_{cat}$) $\gg k_{-1}[Bca]^2$ when [Bca] <20 μM, the second term, $k_{-1}[Bca]^2$, may be ignored under such conditions, and K_m becomes k_2/k_1 (Table 2). Under optimal catalytic conditions as a cuprous oxidase (Scheme 2) and as a phenol oxidase (Scheme 1), the substrate specificity (or catalytic efficiency) may be defined by k_{cat}/K_m. The value is more than 40-fold higher for the former function than for the latter function (under conditions of [Bca] <20 μM; Table 2). Therefore, under the stress of excess Cu^+, CueO can rapidly and specifically catalyze its safe oxidation to less-toxic Cu^{2+}.

Another Cu^I chromophoric ligand, bathocuproine disulfonate anion (Bcs), stabilizes Cu^I with high affinity as an orange complex anion $[Cu^I(Bcs)_2]^{3-}$ ($\lambda_{max} = 483$ nm; $\epsilon = 13\,000$ M^{-1} cm^{-1}; $\beta_2 = 10^{19.8}$ M^{-2})[30] and may be useful as a substrate model for higher affinity Cu^I enzymes. However, CueO was unable to catalyze the air oxidation of $[Cu^I(Bcs)_2]^{3-}$ under conditions equivalent to Figure 6. Like Bca, Bcs exchanges Cu^I with or extracts Cu^I from various proteins rapidly, and there should be little kinetic barrier in Cu^I exchange or extraction involving ligand Bcs.[22,30−32] The reduction potentials of $[Cu^I(Bca)_2]^{3-}$ and $[Cu^I(Bcs)_2]^{3-}$ are similar (Figure S6, Supporting Information). Therefore, lack of reaction with $[Cu^I(Bcs)_2]^{3-}$ as substrate must be attributed to an unfavorable thermodynamic gradient for Cu^I transfer from $[Cu^I(Bcs)_2]^{3-}$ to T4 in CueO. It is instructive that Bcs buffers $[Cu^+]$ concentrations at sub-femtomolar concentrations, matching those of cytosolic Cu^I binding proteins, while Bca buffers $[Cu^+]$ concentrations at sub-picomolar concentrations, comparable to those of periplasmic Cu^I binding proteins.[24]

The affinity of the T4 site in CueO for Cu^I matches those of several bacterial periplasmic Cu^I binding proteins, including CopC, PcoC, and CopK ($\sim 10^{-13}$ M).[21,25,26] These proteins are expressed in response to copper stress and are involved in copper resistance.[1,33] Consequently, they are potential cuprous substrates for enzymes such as CueO, CopA, and PcoA.[15] Preliminary experiments support the reaction model (Scheme 2) derived from study of the model system of CueO/$[Cu^I(Bca)_2]^{3-}$. CueO

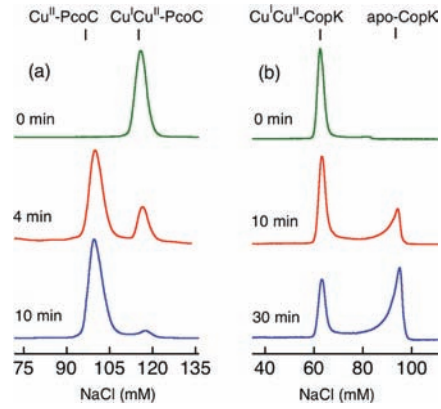

Figure 9. (a) Oxidation of Cu^ICu^{II}-PcoC (50 μM) catalyzed by CueO (1 μM) in air-saturated Mops buffer (20 mM, pH 7.0). The same reaction in BisTris buffer was too rapid to be followed. (b) Oxidation of Cu^ICu^{II}-CopK (50 μM) catalyzed by CueO (1 μM) in air-saturated BisTris buffer (20 mM, pH 7.0). There was no reaction in Mops buffer under the same conditions. The progress of the reactions was analyzed on a Mono-S HR 5/5 cation-exchange column at the indicated reaction times. Oxidation of Cu^ICu^{II}-CopK led to a loss of both Cu^I and Cu^{II}, while oxidation of Cu^ICu^{II}-PcoC led to a loss of Cu^I only.[25] The elution peak intensities have been normalized for clarity.

catalyzed quantitative air oxidation of Cu^ICu^{II}-PcoC ($\sim$50 equiv) in BisTris buffer in <2 min and almost complete oxidation in Mops buffer in $\sim$10 min (Figure 9a). Reaction with Cu^ICu^{II}-CopK was much less efficient under the same conditions. In Mops buffer, there was no apparent catalytic oxidation of Cu^ICu^{II}-CopK for at least 2 h, while in BisTris buffer, the oxidation rate for Cu^ICu^{II}-CopK was lower than that for Cu^ICu^{II}-PcoC by a factor of at least 100 (Figure 9b). Direct equilibrium competitions between PcoC and CopK have demonstrated that these two proteins bind Cu^I with indistinguishable affinities.[25] Hence, the difference in their reactivities toward CueO must be attributed to kinetic rather than thermodynamic effects. The Cu^I site of PcoC lies on a flexible methionine-rich metal binding loop on the protein surface[21,34] and appears to interact efficiently with the methionine-rich T4 site of CueO. In contrast, Cu^I in CopK is bound in a hydrophobic core sandwiched between two β sheets,[25] and this may not allow favorable intermolecular contact with CueO. These differences in reactivity between PcoC and CopK were also observed with cuprous oxidase PcoA, a homologue of CueO also featuring a methionine-rich insert.[15,25] PcoC, but not CopK, is likely to be a physiological partner of PcoA. We are developing sensitive probes to quantitate reactions such as those discussed above.

Concluding Remarks. Most MCOs exhibit broad substrate specificity toward organic reductants, while a few so-called metallo-oxidases are also able to oxidize low-valent first-row transition metal ions such as Fe^{II}, Cu^I, and Mn^{II}.[5] Well-characterized examples of ferrous oxidases include human ceruloplasmin and yeast Fet3p, which are essential for iron metabolism.[35−37] The activity may be attributed to the presence of a (T4) metal binding site specific for Fe^{II} near the T1 copper

(30) Xiao, Z.; Loughlin, F.; George, G. N.; Howlett, G. J.; Wedd, A. G. *J. Am. Chem. Soc.* **2004**, *126*, 3081–3090.
(31) Zimmermann, M.; Xiao, Z.; Cobbett, C. S.; Wedd, A. G. *Chem. Commun.* **2009**, 6364–6366.
(32) Zhou, L.; Singleton, C.; Le Brun, N. E. *Biochem. J.* **2008**, *413*, 459–465.
(33) Monchy, S.; Benotmane, M. A.; Wattiez, R.; van Aelst, S.; Auquier, V.; Borremans, B.; Mergeay, M.; Taghavi, S.; van der Lelie, D.; Vallaeys, T. *Microbiology* **2006**, *152*, 1765–1776.
(34) Wernimont, A. K.; Huffman, D. L.; Finney, L. A.; Demeler, B.; O'Halloran, T. V.; Rosenzweig, A. C. *J. Biol. Inorg. Chem.* **2003**, *8*, 185–194.
(35) Zaitseva, I.; Zaitsev, V.; Card, G.; Moshkov, K.; Bax, B.; Ralph, A.; Lindley, P. *J. Biol. Inorg. Chem.* **1996**, *1*, 15–23.
(36) De Silva, D. M.; Askwith, C. C.; Eide, D.; Kaplan, J. *J. Biol. Chem.* **1995**, *270*, 1098–1101.
(37) Askwith, C.; Eide, D.; Van Ho, A.; Bernard, P. S.; Li, L.; Davis-Kaplan, S.; Sipe, D. M.; Kaplan, J. *Cell* **1994**, *76*, 403–410.

center.[35,38−40] These ferroxidases also possess cuprous oxidase activity because the Fe^{II}-specific T4 site may also bind Cu^{I} with some alternative residues as metal ligands.[41,42]

CueO is a MCO involved in copper efflux in *E. coli*. It exhibits both phenol oxidase and cuprous oxidase activities but with distinctly different reaction mechanisms (Schemes 1 and 2). As a phenol oxidase, a T4 copper atom must be in place to mediate electron transfer between the buried T1 copper center and the organic substrates. However, the lability of this copper center restricts optimal phenol oxidase activity to the 10^{-6}−10^{-9} M concentration range for available Cu_{aq}^{2+}. This suggests that CueO cannot function as a phenol oxidase *in vivo*.

As a cuprous oxidase for oxidation of Cu^{I} bound in ligands or proteins, the T4 site must be vacant to dock Cu^{I}. This site promotes cuprous oxidase activity in at least three ways: (i) its high affinity for Cu^{I} ($K_D = 1.3 \times 10^{-13}$ M) ensures a favorable thermodynamic gradient to recruit Cu^{I} from cuprous substrates; (ii) its modest affinity for Cu^{II} ($K_D = 5.5 \times 10^{-9}$ M) allows fine-tuning of the redox potential of the T4 copper to favor oxidation and elimination of product; and (iii) its proximity to the T1 copper center with a hydrogen bond connecting the two sites provides an efficient pathway for electron transfer (Figure 1b). However, it is a precondition that the substrate and the enzyme must be able to interact directly to facilitate ready transfer of Cu^{I} to the T4 site. These aspects were demonstrated quantitatively in this work for the first time with a robust model substrate $[Cu^{I}(Bca)_2]^{3-}$ and two bacterial periplasmic Cu^{I} binding proteins, PcoC and CopK. The results provide compelling evidence that CueO is a cuprous oxidase *in vivo*, not a phenol oxidase. The new approach will have general application to study of the reaction mechanisms of metallo-oxidase enzymes.

Experimental Section

Materials. Chemicals and reagents (analytical grade) were purchased from Sigma. Stock solutions of $[Cu^{I}(Bca)_2]^{3-}$ and $[Cu^{I}(Bcs)_2]^{3-}$ were prepared anaerobically in a glovebox ($[O_2] < 2$ ppm) by addition of $[Cu^{I}(CH_3CN)_4]ClO_4$ in CH_3CN into solutions of Na_2L (L= Bca or Bcs) in Mops buffer (50 mM, pH 7.0) with varying molar ratios of Cu^{I}:L. The Cu^{I} concentration was calibrated by the absorbance of these anions, while Bca and Bcs concentrations were calibrated by titration with a Cu^{2+} standard in the presence of weak reductant NH_2OH, as detailed previously.[21] Buffers or reaction solutions were saturated with air by bubbling, and the $[O_2]$ concentration was assumed to be 285 μM.[43]

Construction of Expression Plasmid and Mutagenesis. Genomic DNA was isolated from *E. coli* strain DH5α using the Wizard Genomic DNA purification kit (Promega). The 1.5 kb gene fragment encoding the mature CueO protein without the N-terminal leader sequence (the first 28 residues) was amplified by polymerase chain reaction with primers designed from the reported CueO gene sequence[11] (P1, 5′-CGGAATTCCCATGGCAGAACGCCCAACGTTACCGATCCCTG-3′; P2, 5′-AAACTGCAGGGATCCTTATACCGTAAACCCTAACATCATCCCCGTATC-3′). Restriction sites *Nco*I and *Bam*HI (underlined) were introduced into the forward and reverse primers, respectively, to facilitate cloning into the expression vector pET-11d (Novagen). Correct insert of CueO gene was confirmed by DNA sequencing.

Protein Expression and Purification. The expression plasmid was transformed into *E. coli* strain BL21(DE3) Codon-Plus(+) cells (Novagen) for protein expression. Cell culture in 2YT rich medium containing ampicillin (100 mg/L) and chloramphenicol (34 mg/L) was shaken at 37 °C until cell optical density at 600 nm reached about 1. The culture was cooled to <30 °C, and IPTG was added to a final concentration of 0.1 mM to induce protein expression. Following further incubation at ambient temperature for 12−16 h, cells were harvested by centrifugation at 4 °C. A clarified cell extract was prepared in Tris-HCl buffer (20 mM; pH 8.5) containing EDTA (1 mM) and glycerol (5−10%) in a total volume of ∼40 mL per gram of wet cells and was applied to an anion-exchange DE-52 (Whatman) column. After the column was washed with the same buffer, the bound proteins were eluted using a NaCl gradient of 0−200 mM in the same buffer. Fractions containing CueO were identified by phenol oxidase activity assay and/or SDS−PAGE and were pooled and concentrated. The final purification step used a Superdex-75 gel filtration column (HR16/60, Amersham Bioscience) with Mops buffer (20 mM, pH 7; 100 mM $NaNO_3$) to remove EDTA and minor components of other contaminant proteins. The purity and identity of the isolated CueO protein were confirmed by SDS−PAGE and ESI−QTOF (Figure S1). The protein was isolated in *apo*-form and was concentrated with glycerol (∼10%) to prevent precipitation at high protein concentration.

Bacterial periplasmic proteins PcoC and CopK that bind both Cu^{I} and Cu^{II} at two separate sites were isolated as reported previously.[21,25]

Copper Incorporation and Analysis. A blue solution was obtained upon stepwise titration of $CuSO_4$ (20 mM, ∼10 equiv) into a stirred solution of *apo*-CueO (0.2−0.3 mM) in Mops buffer (50 mM, pH 7.0; GSH, 1 mM). After incubation at 4 °C for 1−2 h, excess copper ions and reductant were removed by buffer exchange through a Bio-Del P-6 DG gel desalting column (Bio-Rad) in Mops buffer (50 mM, pH 7.0) to produce sample Cu^{II}-CueO (Figure 2b). Equivalent procedures but with the desalting Mops buffer containing BisTris-HCl (10 mM) produced □-CueO (Figure 2a).

Protein concentrations were estimated from their solution spectra using $\epsilon_{280} = 55\,920\ M^{-1}\ cm^{-1}$ for *apo*-CueO estimated from the protein sequence and $\epsilon_{610} = 5000\ M^{-1}\ cm^{-1}$ for *holo*-CueO. Copper content in *holo*-CueO was estimated using Bcs as a chromophoric ligand for Cu^{I} following published procedures in the presence of guanidinium hydrochloride (6 M) and dithionite (250 μM).[44]

Phenol Oxidase Activity. Steady-state kinetic studies were performed by spectroscopic monitoring of the air oxidation of DMP (0.5−20 mM) catalyzed by Cu^{II}-CueO (0.1 μM) in air-saturated Mops buffer (50 mM, pH 7) in a mixing cell. Oxidation produced brown dimeric compound TMPQ, which exhibited an absorption maximum at 469 nm ($\epsilon = 14\,800\ M^{-1}\ cm^{-1}$).[45] The reaction was prepared by loading each half of the mixing cell with equal volumes of DMP and CueO enzyme solutions separately. After zeroing the baseline at 469 nm, the reaction was initiated by rapid mixing of the two solutions, and the increase in A_{469} was followed for 5 min (Figure S2). Initial steady-state DMP consumption rates (expressed as molecular velocity in unit of min^{-1}) were calculated and kinetic parameters K_m and k_{cat} derived by direct fitting to the Michaelis−Menten equation.

Studies of the effects of different buffers on the activity were conducted by loading DMP (20 mM) in each buffer tested in one half-cell and the Cu^{II}-CueO enzyme (0.2 μM) in Mops in the other half-cell (note that the concentrations were halved after mixing). Studies of the effects of added Cu^{2+} were carried out by preloading

(38) Taylor, A. B.; Stoj, C. S.; Ziegler, L.; Kosman, D. J.; Hart, P. J. *Proc. Natl. Acad. Sci. U.S.A.* **2005**, *102*, 15459–15464.
(39) Lindley, P. F.; Card, G.; Zaitseva, I.; Zaitsev, V.; Reinhammar, B.; Selin-Lindgren, E.; Yoshida, K. *J. Biol. Inorg. Chem.* **1997**, *2*, 454–463.
(40) Stoj, C. S.; Augustine, A. J.; Zeigler, L.; Solomon, E. I.; Kosman, D. J. *Biochemistry* **2006**, *45*, 12741–12749.
(41) Stoj, C. S.; Augustine, A. J.; Solomon, E. I.; Kosman, D. J. *J. Biol. Chem.* **2007**, *282*, 7862–7868.
(42) Stoj, C.; Kosman, D. J. *FEBS Lett.* **2003**, *554*, 422–426.
(43) Atkins, P. W.; de Paula, J. *Physical Chemistry*, 7th ed.; Freeman: New York, 2002.
(44) Blair, D.; Diehl, H. *Talanta* **1961**, *7*, 163–174.
(45) Slomczynski, D.; Nakas, J. P.; Tanenbaum, S. W. *Appl. Environ. Microbiol.* **1995**, *61*, 907–912.

the Cu^{2+} with Cu^{II}-CueO in one half-cell and DMP in a suitable buffer in the other half-cell.

Affinity of the T4 site for Cu^{II}. Phenol oxidase activity of CueO is proportional to the Cu^{II} occupancy on the T4 site, which may be controlled by a Cu^{2+} buffer composed of Cu^{II}-BisTris and BisTris (see eq 2). For a series of BisTris-HCl solutions (50 mM, pH 7.0) containing increasing amounts of total Cu^{II} ions (5−200 μM), the $[Cu^{2+}]$ concentrations were calculated from the reported apparent $K_D(Cu^{II}) = 10^{-5.14}$ for BisTris at pH 7.[17] In these solutions, the phenol oxidase activity increased with increasing total Cu^{II} concentration until reaching a value comparable to the optimal activity (v_{max}) observed in pure Mops buffer without added excess Cu^{2+}. A plot of log $[(v/v_{max})/(1 - v/v_{max})]$ versus log $[Cu^{2+}]$ generated a straight line. Log $K_D(Cu^{II})$ for the T4 site is the log $[Cu^{2+}]$ value that corresponds to half-maximal activity (Figure 4a inset). Controls without CueO confirmed that added Cu^{2+} in BisTris buffer induced only insignificant background oxidation.

Cuprous Oxidase Activity. Several cuprous substrates were employed for the assay, including $[Cu^{I}(CH_3CN)_4]^{+}$, $[Cu^{I}(Bca)_2]^{3-}$, $[Cu^{I}(Bcs)_2]^{3-}$, $Cu^{I}Cu^{II}$-PcoC, and $Cu^{I}Cu^{II}$-CopK. The assay approaches varied with substrate properties. With $[Cu^{I}(CH_3CN)_4]^{+}$ as substrate, the reaction was followed indirectly by monitoring O_2 consumption with a Clark-type oxygen sensor electrode (Unisense, Denmark). Briefly, a reaction vial (~1.6 mL) containing the oxygen electrode was filled completely with an air-saturated buffer solution containing CueO enzyme (0.25 μM) and CH_3CN (~10%). After the electrode response stabilized, a small volume (<160 μL) of an anaerobic solution of $[Cu^{I}(CH_3CN)_4]^{+}$ in CH_3CN was added under stirring to start the reaction. Change in oxygen concentration in the solution was monitored using OXYgraph (Unisense, Denmark) for about 30 min. Controls were carried out in the absence of the CueO enzyme.

Equivalent experiments using the oxygen electrode were performed with $[Cu^{I}(Bca)_2]^{3-}$ (100−200 μM) as a substrate in Tris-HCl buffer (50 mM, pH 7.0), but with a slightly different procedure. The reaction vial was preloaded with $[Cu^{I}(Bca)_2]^{3-}$ in air-saturated buffer and sealed with a rubber cap to minimize air exposure. After the electrode response became stable, the cap was lifted briefly to introduce the CueO enzyme (0.25−2.0 μM) to initiate the reaction. However, a more convenient and reliable approach involves direct monitoring of the change in absorbance of $[Cu^{I}(Bca)_2]^{3-}$ at 562 and/or 480 nm,[22] depending on the initial substrate concentration (see Figures S4 and S5). Oxidation of the bound Cu^{I} led to loss of the color and dissociation of the Cu^{2+} ion. Effects of buffer compositions and metal ions on the cuprous oxidase activity were investigated with an enzyme concentration of 1.0 μM and substrate $[Cu^{I}(Bca)_2]^{3-}$ concentration of ~100 μM. The reactions were conducted in the mixing cell as detailed above.

The steady-state kinetic assay of cuprous oxidase activity on $[Cu^{I}(Bca)_2]^{3-}$ was performed in air-saturated BisTris-HCl buffer (50 mM, pH 7) with CueO (0.1 μM) and $[Cu^{I}(Bca)_2]^{3-}$ (25−500 μM). The initial substrate concentration for each reaction was confirmed by A_{562} before mixing the solutions and starting the reaction. Since the oxidation rate is accelerated with increasing substrate $[Cu^{I}(Bca)_2]^{3-}$ concentration, but is suppressed by free Bca which is produced constantly during the course of the oxidation, two types of experiments were designed and executed. The first consisted of experiments with a series of substrate solutions containing varying concentrations of [Bca] and $[Cu^{I}(Bca)_2]^{3-}$, but with the same molar ratio of these two species at reaction points where the reaction rates were recorded and calculated. This was achieved by preparing the solution series from dilutions of the same solution stock which contained a molar ratio $Bca:Cu^{I} = 2.5:1.0$ (i.e., $[Bca]:[Cu^{I}(Bca)_2^{3-}] = 0.50:1.0$). The reaction rate for each reaction was recorded and calculated at the reaction point of oxidation of 10% initial $[Cu^{I}(Bca)_2]^{3-}$, and thus $[Bca]:[Cu^{I}(Bca)_2^{3-}]$ became 0.78:1.0. This ratio was used for curve-fitting, and the result is shown in Figure 6a. The second type of experiments measured and compared reaction rates with solution series that contained identical $[Cu^{I}(Bca)_2^{3-}]$ but varying $[Bca]_{free}$ (Figure 6b). Steady-state reaction rates expressed as molecular velocity (min^{-1}) were calculated, and the kinetic parameter ($n - m$) was derived from curve-fitting of the data in Figure 6b to eq 7. The other parameters (i.e., k_1, k_{-1}, and k_{cat}) were subsequently derived by direct fitting of all experimental data to eq 7 with a fixed value ($n - m$) = 2 as defined.

Oxidation of $[Cu^{I}(Bcs)_2]^{3-}$ (25−50 μM) catalyzed by CueO (2.0 μM) was monitored at 483 nm. Oxidation of $Cu^{I}Cu^{II}$-PcoC and $Cu^{I}Cu^{II}$-CopK was analyzed by an analytical cation-exchange column as detailed previously.[15]

Electrochemistry of $[Cu^{I}L_2]^{3-}$ (L = Bca, Bcs). Electrochemical experiments were performed using a standard three-electrode system. The working electrode was a disc (d = 5 mm) of edge-cleaved pyrolytic graphite (PGE, Le Carbone-Lorraine) housed in a sheath of epoxy resin. The electrode was polished manually using a slurry of alumina (0.3 μm) in water and rinsed with distilled water. The counter electrode was a Pt wire. Observed potentials are quoted relative to the standard hydrogen electrode (SHE) and were measured relative to a KCl-saturated Ag/AgCl reference electrode (197 mV vs SHE at 25 °C). Potentials were calibrated with the methyl viologen couple (−446 mV vs SHE at 25 °C). The working solutions of $[Cu^{I}(Bca)_2]^{3-}$ and $[Cu^{I}(Bcs)_2]^{3-}$ (each 1.0 mM in [Cu] with $[L]/[Cu] \geq 3$) were prepared in a KPi buffer (50 mM, pH 7; NaCl, 100 mM). Dioxygen was removed by bubbling water-saturated dinitrogen through the solution before each experiment.

Abbreviations Used. aa, amino acid; Bca, bicinchoninic acid anion; Bcs, bathocuproine disulfonate anion; BisTris, 2-[bis(2-hydroxyethyl)amino]-2-(hydroxymethyl)-l,3-propanediol; DMP, 2,6-dimethoxyphenol; EDTA, ethylenediamine-*N*,*N*,*N*′,*N*′-tetraacetic acid; eq, equation; equiv, equivalent; GSH, glutathione; IPTG, isopropyl-β-D-thiogalactopyranoside; NaAc, sodium acetate; KPi, potassium phosphate buffer; MCO, multicopper oxidase; Mops, 3-(*N*-morpholino)propanesulfonic acid; NaAc, sodium acetate; TMPQ, 3,5,3′,5′-tetramethoxydiphenoquinone; Tris, tris(hydroxymethyl)aminoethane.

Acknowledgment. We thank the Australian Research Council for financial support under Grant A29930204.

Supporting Information Available: Protein characterization data (ESI-MS, Figure S1), catalytic reactions (Figures S2−S5), and cyclic voltammetry (Figure S6). This material is available free of charge via the Internet at http://pubs.acs.org.

JA9091903